

## CHAPTER-6

*X-ray diffraction studies and refractive index measurements on a mesomorphic mixture showing enhanced smectic  $A_d$  phase and re-entrant nematic phase.*

The phase diagrams of the mixtures of 4 - cyanobiphenyl -4' alkyl biphenyl - 4 - carboxylates (nCBB) and alkyloxy - 4' - cyanobiphenyls (nOCB) have been studied extensively by Brodzik and Dabrowski [1]. Some of these mixtures have very interesting property of showing induced smectic  $A_d$  phase as well as re-entrant nematic phase in a particular composition range. Some of the mixtures even produce a smectic  $A_d$  island in a nematic sea. Hence, these mixtures are well suited for the study of physical properties, which may elucidate the formation of induced smectic  $A_d$  phases and re-entrant nematic phases in these mixtures.

The mixtures of 4 - cyanobiphenyl -4' heptyl biphenyl - 4 - carboxylate (7CBB) and 4 - dodecyloxy- 4 - cyanobiphenyl (12OCB) have been studied by us. Figure 6.1 shows the phase diagram of this mixture as obtained by Brodzik et al.[1]. This system shows enhanced smectic  $A_d$  phase as well as re-entrant nematic phase. Whereas, in 12OCB the smectic  $A_d$  phase is stable only upto  $88.5^\circ\text{C}$ , in this mixture at optimum composition the smectic  $A_d$  phase can exist upto  $264^\circ\text{C}$ . Due to this unusual properties we decided to study this mixture by small angle x-ray diffraction technique and also to measure the density and refractive index of this mixture.

The pure compounds were prepared at the Institute of Chemistry, Military University of Technology, Warsaw. Mixtures were prepared at Physics Department, North Bengal University, where the X-ray diffraction studies and refractive index measurements were performed. Mixtures of 12OCB and 7CBB were prepared with six different compositions all in the range showing enhanced smectic  $A_d$  phase. One of the mixtures, having mole fraction of 0.917 of 7CBB, showed re-entrant nematic phase as well. The transition temperature of the mixtures were determined by observing

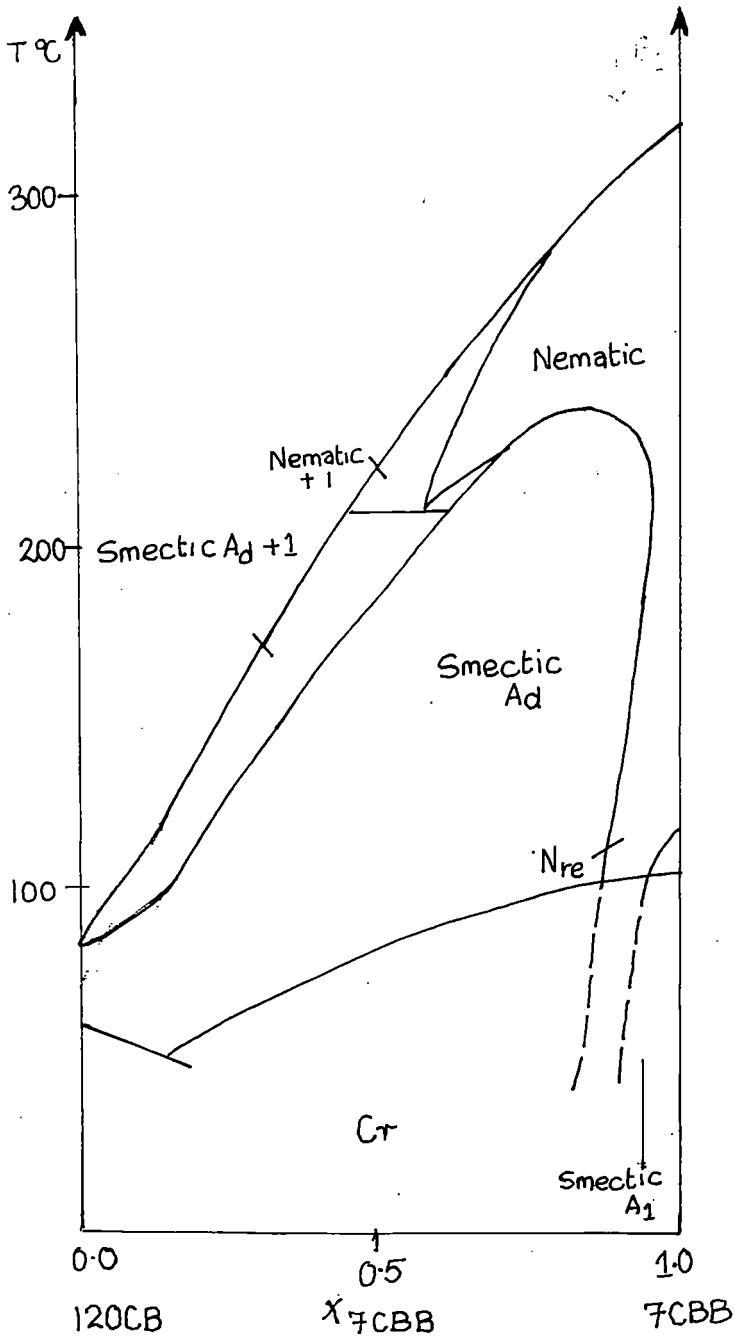
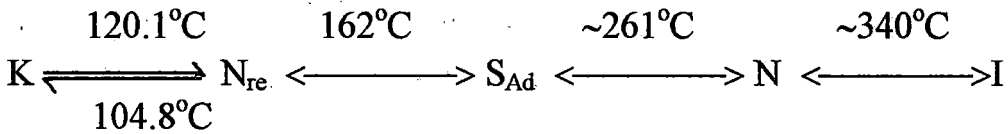


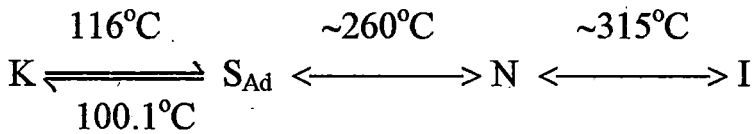
Figure 6.1. Phase diagram of bicomponent mixture (7CBB and 12OCB).

textures under polarising microscope, using Mettler FP 80/82 thermosystem. Unfortunately, at higher temperatures the components decompose, so no high temperature ( $>200^{\circ}\text{C}$ ) experiments could be performed on these mixtures. The composition of mixtures studied were  $x_{7\text{CBB}} = 0.917$  (mix.  $C_1$ ),  $0.80$  (mix.  $C_2$ ),  $0.604$  (mix.  $C_3$ ),  $0.502$  (mix.  $C_4$ ),  $0.296$  (mix.  $C_5$ ),  $0.202$  (mix.  $C_6$ ),  $x_{7\text{CBB}}$  being the mole fraction of 7CBB. The method of refractive index and density measurements and the details of x-ray diffraction set-up used have been described in Chapter 2. Since, mixture  $C_1$ , having mole fraction  $0.917$  of 7CBB, shows both enhanced smectic  $A_d$  and re-entrant nematic phases, we studied this mixture more thoroughly. The transition temperatures of the mixtures as observed by us are given below:

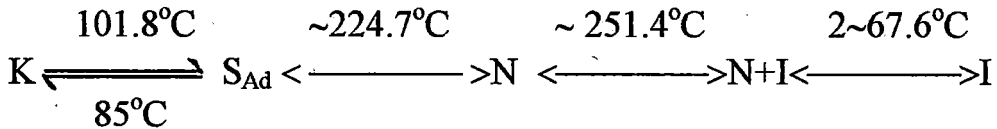
I. Mix.  $C_1$



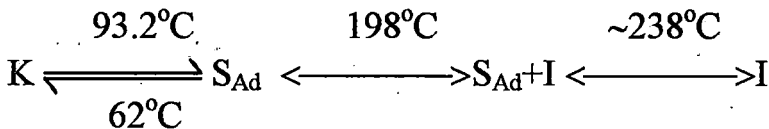
II. Mix.  $C_2$

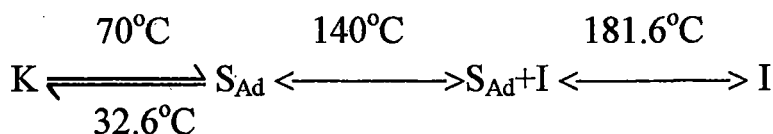
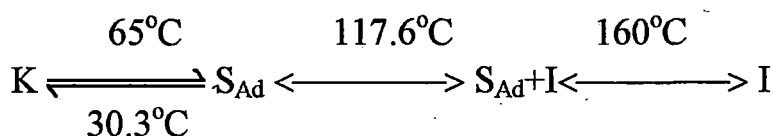


III. Mix.  $C_3$



IV. Mix.  $C_4$



V. Mix. C<sub>5</sub>VI. Mix. C<sub>6</sub>

All the transition temperatures agree with the values obtained from the phase diagram [1] for this mixture. The densities and the values of ordinary and extraordinary refractive indices at three different wave lengths (5461 Å, 5780 Å and 6907 Å) for mixture C<sub>1</sub> in the temperature range 120°C to 175 °C have been tabulated in Table 6.1. Above 175 °C the sample started to decompose, so experimental data at higher temperatures could not be taken. The temperature variation of the density for mixture C<sub>1</sub> is shown in Figure 6.2. No discontinuity in the density value could be observed at the re-entrant nematic to smectic A<sub>d</sub> phase. Hence, this phase transition is probably of the second order. The temperature variation of the ordinary and extraordinary refractive indices at three different wavelengths is given in Figure 6.3. It can be seen that refractive indices also vary continuously across the re-entrant nematic to smectic A<sub>d</sub> phase transition. The polarisability values calculated according to Vuks formula (equation 2.24 & 2.25) and Neugebauer formula (equation 2.22 & 2.23) are given in Tables 6.2 and 6.3 respectively. The polarisability and anisotropies in the perfectly ordered state are determined by Haller's extrapolation method. The order parameters calculated using Vuks and Neugebauer procedure are given in Tables 6.4 and 6.5 respectively. Though the two methods give quite different values of  $\Delta\chi (= \chi_{\parallel} - \chi_{\perp})$ , the order parameter values agree

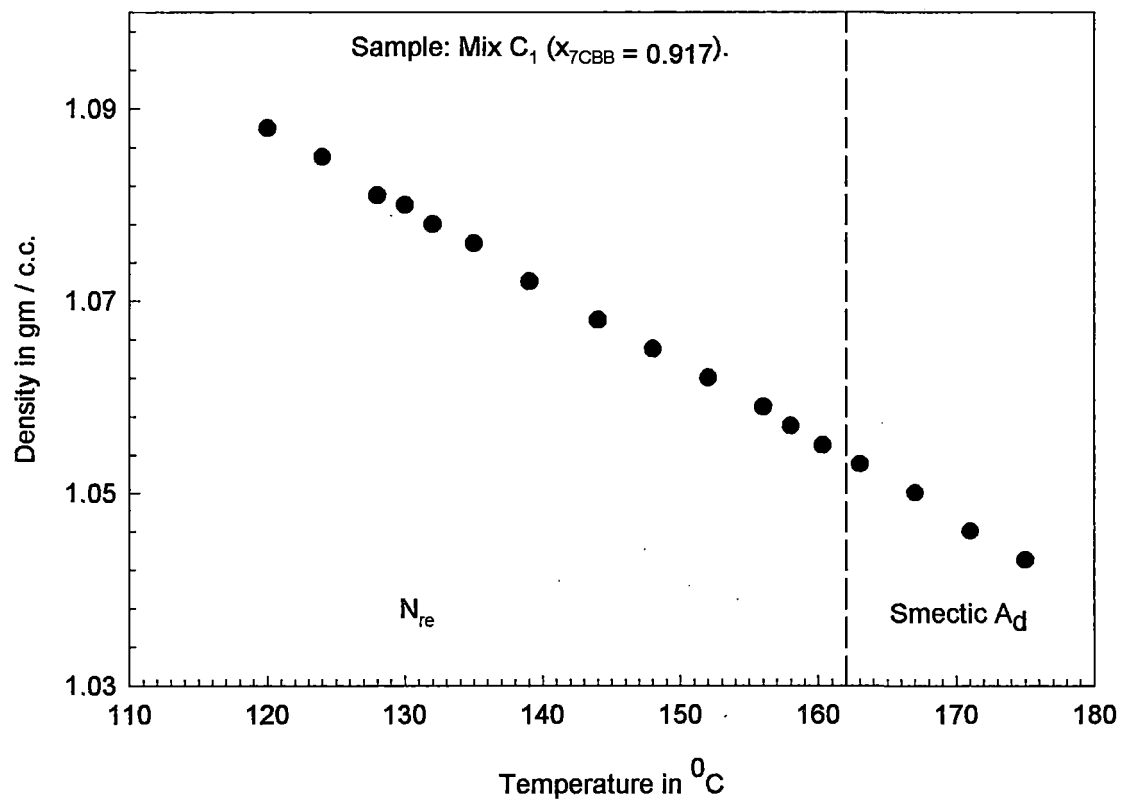


Figure 6.2. Density values as a function of temperature.

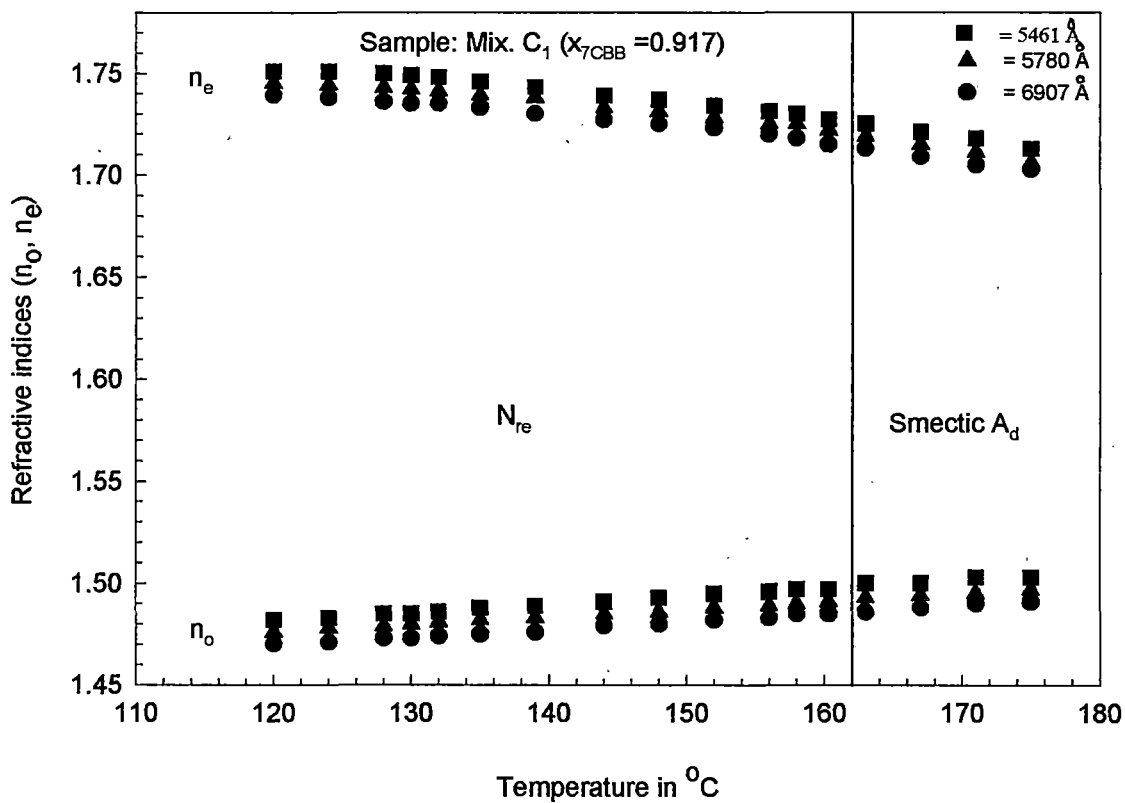


Figure 6.3. Variation of refractive indices ( $n_o, n_e$ ) with temperature.

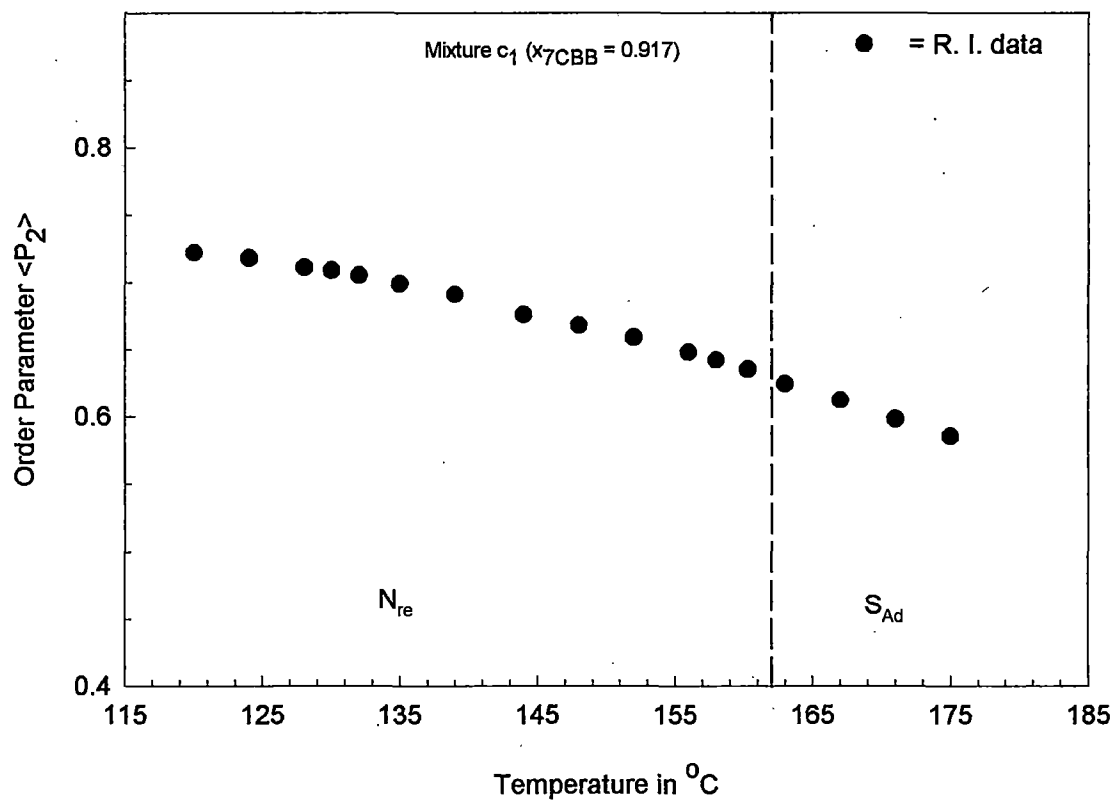
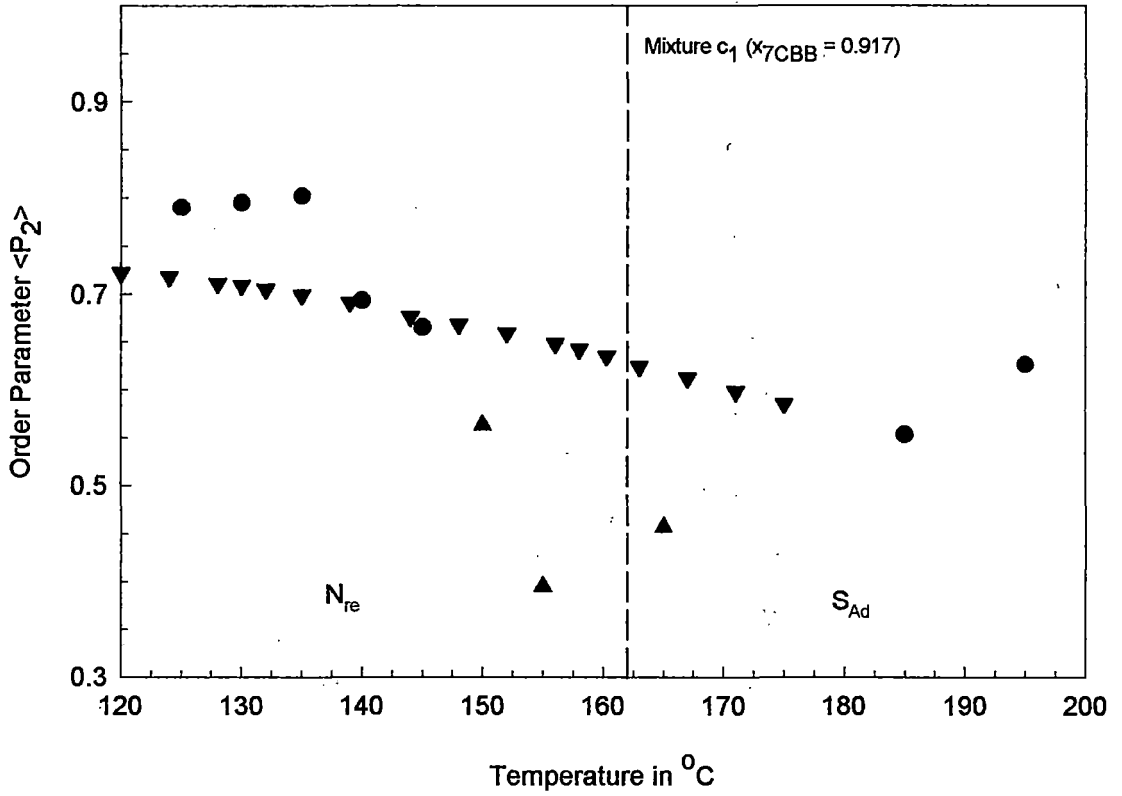


Figure 6.4. Temperature variation of orientational order parameter  $\langle P_2 \rangle$  in the re-entrant nematic and induced smectic  $A_d$  phase.

almost exactly. Figure 6.4 shows the temperature variation of the order parameter as calculated from refractive index data. Again we find that there is no sudden change in the order parameter value at the re-entrant nematic to smectic  $A_d$  phase transition temperature.

X-ray diffraction patterns were recorded for mixture  $C_1$  at ten temperatures between  $125^{\circ}\text{C}$  to  $195^{\circ}\text{C}$ . A magnetic field of 5 kilogauss was applied to align the sample. However, at three temperatures near the re-entrant nematic to smectic  $A_d$  phase transition the sample could only be partially aligned. The sample could be taken to higher temperature ( $195^{\circ}\text{C}$ ) without decomposition, since the sample was sealed in a glass capillary tube, where atmospheric oxygen could not get in to react with the chemicals. In case of refractive index and density measurements, our system was not sealed, hence decomposition set in at a lower ( $\sim 175^{\circ}\text{C}$ ) temperature.

Angular distribution of the intensities of the outer x-ray diffraction pattern after conversion from optical density to x-ray intensity and correction for the background are tabulated in Tables 6.6 and 6.7. These intensity data have been analysed to obtain angular distribution function using Leadbetter [2] procedure and the angular distribution function values are given in Tables 6.8 and 6.9. The order parameters as calculated from the x-ray data for this mixture (mix. $C_1$ ) at different temperatures are tabulated in Table 6.10. Figure 6.5 shows the temperature variation of order parameter for mix. $C_1$  as obtained from x-ray diffraction and refractive index studies. It can be seen that if the  $\langle P_2 \rangle$  values obtained from partially aligned samples be ignored then the agreement between order parameters determined from two different techniques is fair. However, since samples near the  $N_{re}$  - Smectic  $A_d$  transition could not be aligned for x-ray



of orientational order parameter  $\langle P_2 \rangle$  in

diffraction studies, the nature of this phase transition could not be inferred from x-ray studies. But, the density and refractive<sup>index</sup> show that  $N_{re}$  - Smectic  $A_d$  transition is most probably of the second order.

The rest five mixtures have only smectic  $A_d$  and normal nematic phases at high temperature. None of the mixtures in the smectic phase could be aligned in the magnetic field at our disposal ( $\sim 5$  kilogauss). The x-ray diffraction pattern of the normal nematic phase could not be obtained since the sample started to decompose at higher temperatures. Hence, only layer thickness measurements could be done for these mixtures in their smectic  $A_d$  phase from the study of the inner arc of the x-ray diffraction pattern. The layer thickness at different temperatures for all the six mixtures are recorded in Tables 6.11 and 6.12. The apparent molecular lengths in the re-entrant nematic phase of mixture  $C_1$  have also been given in Table 6.11. X-ray diffraction photographs from the mixture  $C_1$  in the re-entrant nematic phase (at  $125^\circ\text{C}$  and  $150^\circ\text{C}$ ) and in the smectic  $A_d$  phase ( $185^\circ\text{C}$ ) are shown in Plates 6a-6c. The temperature variation of apparent molecular length in the re-entrant nematic phase and of layer thickness of the smectic  $A_d$  phase for mixture  $C_1$  is shown in Figure 6.6. It can be seen that the apparent molecular length in the re-entrant nematic phase in mixture  $C_1$  is about  $39.8 \text{ \AA}$ , whereas the layer thickness in the smectic  $A_d$  phase of the same mixture is about  $38.7 \text{ \AA}$ . So there is definite re-arrangement of molecular packing at the phase transition. The apparent molecular length in the  $N_{re}$  phase very near the transition temperature is almost equal to the smectic layer thickness. This may be due to the pre-transitional effect, when smectic like clusters may be forming in the re-entrant nematic phase. Hence, x-ray diffraction from the re-entrant nematic phase near the transition temperature should be very similar to those from

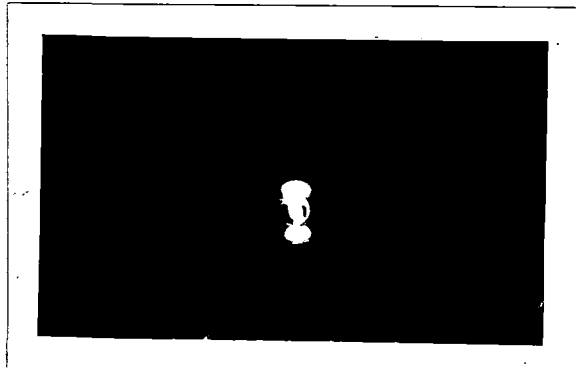


Plate 6a: X-ray diffraction photograph of the oriented sample in the re-entrant nematic phase of 7CBB+12OCB mixture at 125°C.

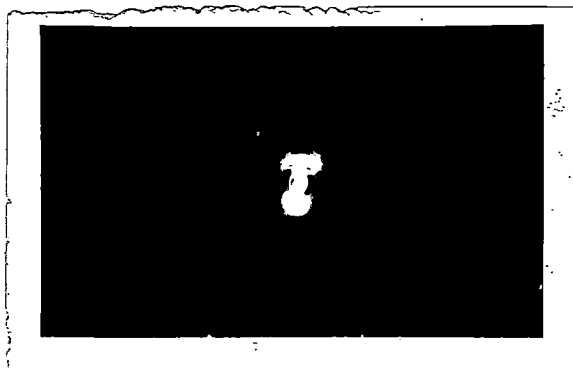


Plate 6b: X-ray diffraction photograph of the oriented sample in the re-entrant nematic phase of 7CBB+12OCB mixture at 125°C.



Plate 6c: X-ray diffraction photograph of the oriented sample in the smectic A<sub>d</sub> phase of 7CBB+12OCB mixture at 185°C.

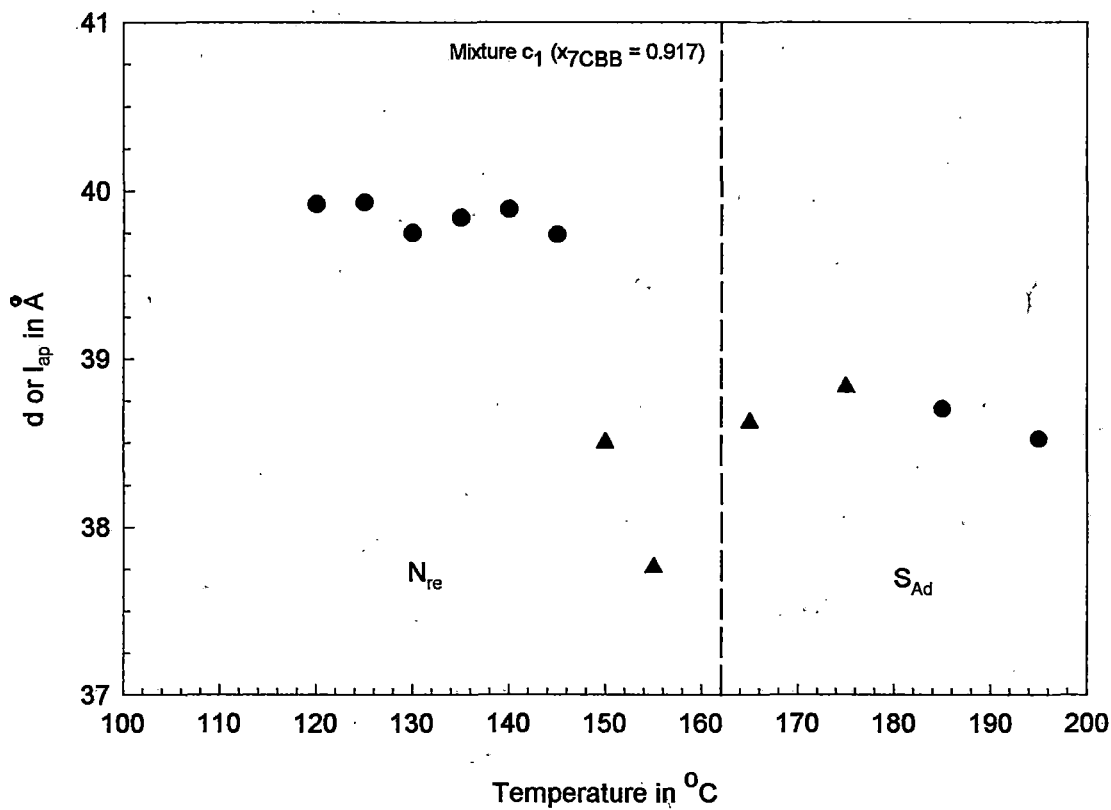


Figure 6.6. Temperature variation of apparent molecular length ( $l_{ap}$ ) in the re-entrant nematic phase and of layer thickness ( $d$ ) in the smectic  $A_D$  phase from x-ray photographs.

- data from aligned sample
- ▲ data from partially aligned sample

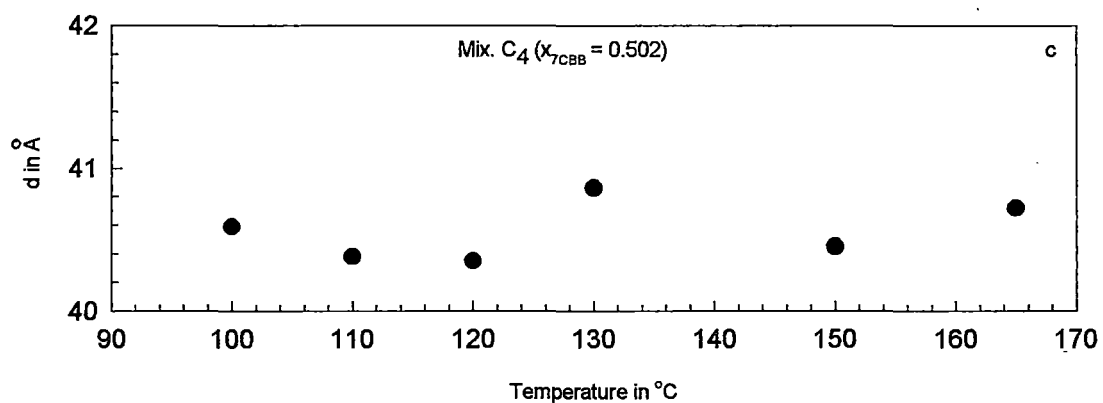
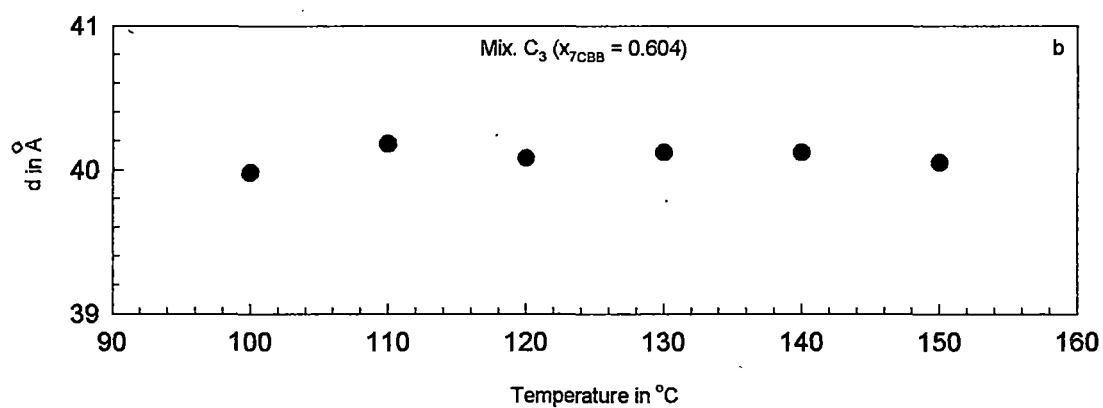
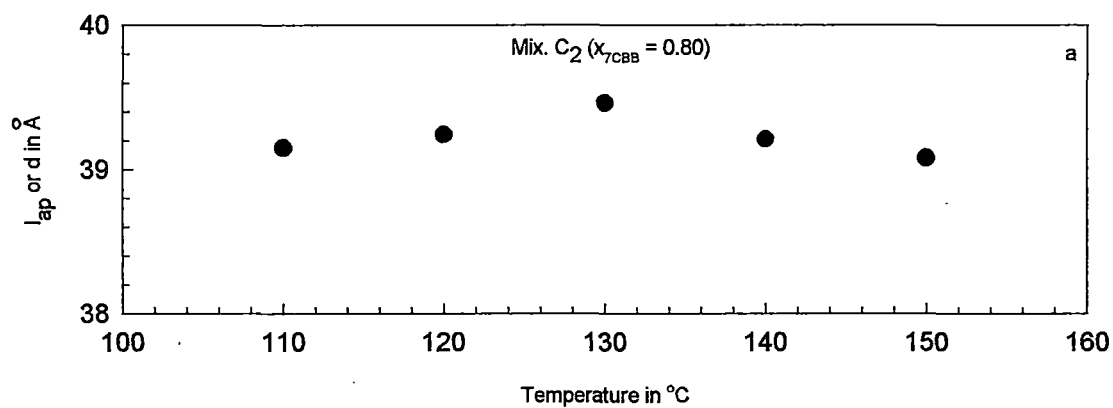


Figure ( 6.7a - 6.7c ). Temperature variation of layer thickness ( $d$ ).

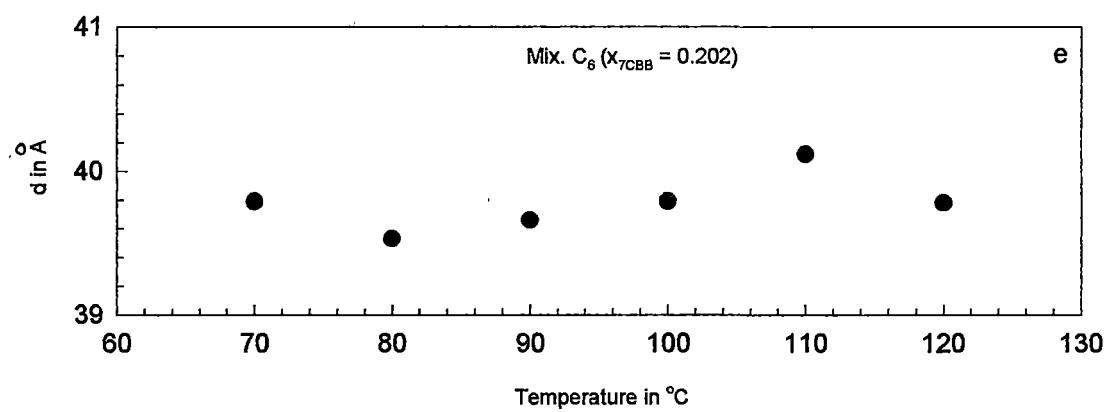
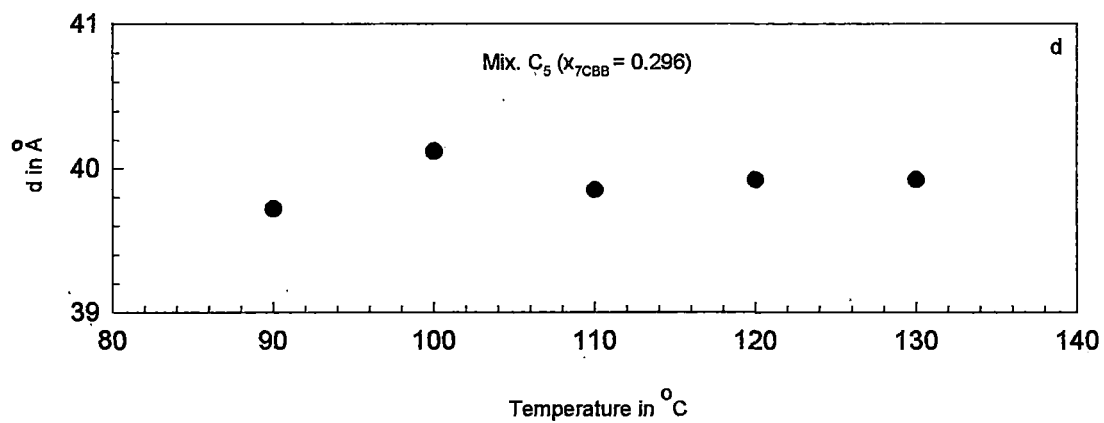


Figure (6.7d - 6.7e). Temperature variation of layer thickness (d).

the smectic  $A_d$  phase. Indeed the x-ray diffraction pattern (Plate 6b) from re-entrant nematic phase of mixture  $C_1$  at  $150^\circ\text{C}$  does show typical inner spots due to cybotactic clusters.

The temperature variation of the layer thickness in the mixture  $C_2$  to mixture  $C_6$  are shown in Figure 6.7a - 6.7e. It can be seen that the layer thicknesses are almost independent of temperature. This is quite common in smectic A phases. The composition variation of layer thickness at  $120^\circ\text{C}$  (except for mixture  $C_1$  for which the layer thickness is at  $170^\circ\text{C}$ ) is shown in Figure 6.8. The variation shows a broad maximum of  $\sim 40\text{\AA}$  at about equimolar concentration. This has already been reported by us [5]. This is in contrast to some polar-nonpolar mixtures [3,4] showing induced smectic  $A_d$  phase, where the layer thickness shows a minimum at about equimolar composition. However, this maximum is not difficult to explain. The model molecular lengths of 7CBB and 12OCB molecules are  $31.5\text{\AA}$  and  $25.6\text{\AA}$  respectively. 7CBB has a latent smectic  $A_1$  phase [1], that means that pure 7CBB, if it forms a smectic phase will have a layer thickness of about  $31.5\text{\AA}$ . 12OCB forms a partial bilayer smectic (i.e. smectic  $A_d$ ) phase of layer thickness  $37.5\text{\AA}$  approximately [6]. However, in the mixture of 7CBB and 12OCB dimer formation between 7CBB and 12OCB will certainly occur. We can assume that in an equimolar mixture 7CBB + 12OCB dimers will predominate in number over 12OCB + 12OCB dimers. The length of 7CBB + 12OCB dimer should be greater than 12OCB + 12OCB dimers and this length should be almost equal to the layer thickness of the smectic phase of equimolar mixture of 7CBB and 12OCB. To estimate the length of 7CBB + 12OCB dimers, we can proceed as follows. The length of 12OCB molecule is  $25.6\text{\AA}$  and that of its dimer is  $37.5\text{\AA}$ , if we assume that the layer thickness in the smectic A phase of 12OCB is equal to its

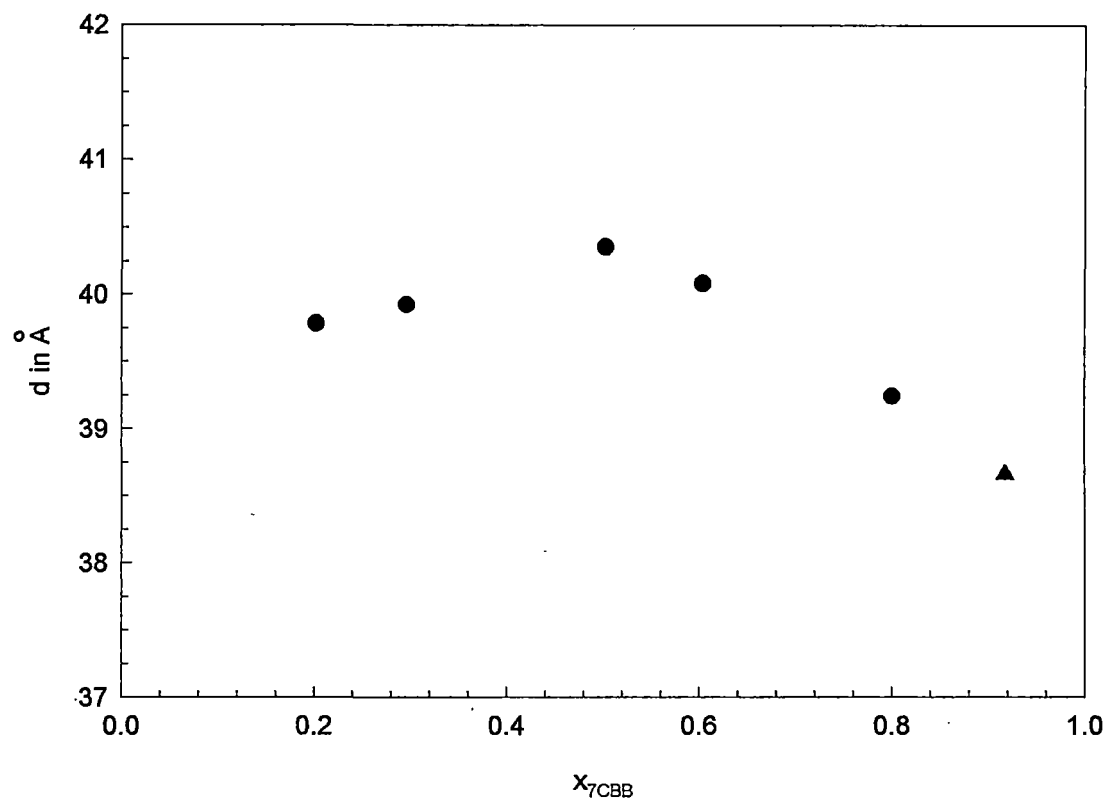


Figure 6.8. Concentration variation of the layer thickness of mixture of 7CBB & 12OCB AT 120 °C { except point  $x_{7CBB} = 0.917$  (  $\blacktriangle$  ) for which temperature is about 170 °C }.

dimer length. Then the overlap of the two 12OCB molecules in the dimer is about  $14\text{\AA}$ . Now 7CBB molecule contains a cyanobiphenyl part identical to that in 12OCB. Since dimer formation is enhanced by the presence of cyanobiphenyl in a molecule, we can assume that in 7CBB + 12OCB dimer an identical overlap of the molecules ( $16\text{\AA}$ ) takes place as in 12OCB + 12OCB dimer. Hence, the length of 7CBB + 12OCB dimer comes out to be  $31.5\text{\AA} + 25.6\text{\AA} - 14\text{\AA} = 43.1\text{\AA}$ . This value is slightly greater than the maximum value of the layer thickness ( $\sim 40\text{\AA}$ ) observed in the mixture of 7CBB and 12OCB. If we consider the presence of 12OCB dimers and some 7CBB monomers then the mean layer thickness should be reduced somewhat from  $43.1\text{\AA}$ . As the composition changes from equimolar, the number of 7CBB + 12OCB dimers reduces and 12OCB + 12OCB dimers increases. Since the 12OCB dimers ( $37.5\text{\AA}$ ) are shorter than 7CBB + 12OCB ( $43.1\text{\AA}$ ) dimers, it means that the effective layer thickness should be maximum for equimolar mixture. This is exactly what is seen in Figure 6.8. Further work is in progress to explain quantitatively this variation of layer thickness with mole fraction.

**Table 6.1**

**Density ( $\rho$ ) and refractive indices ( $n_o$ ,  $n_e$ ) at different temperatures of mixture  $C_1$  ( $x_{7CBB} = 0.917$ ) of 7CBB and 12OCB.**

Temp. in °C	Density in gm/cc	$\lambda = 6907 \text{ \AA}$		$\lambda = 5780 \text{ \AA}$		$\lambda = 5461 \text{ \AA}$	
		$n_o$	$n_e$	$n_o$	$n_e$	$n_o$	$n_e$
120	1.088	1.470	1.739	1.476	1.745	1.482	1.751
124	1.085	1.471	1.738	1.478	1.744	1.483	1.751
128	1.081	1.473	1.736	1.479	1.743	1.485	1.750
130	1.080	1.473	1.735	1.480	1.742	1.485	1.749
132	1.078	1.474	1.735	1.481	1.741	1.486	1.748
135	1.076	1.475	1.733	1.482	1.739	1.488	1.746
139	1.072	1.476	1.730	1.483	1.738	1.489	1.743
144	1.068	1.479	1.727	1.485	1.733	1.491	1.739
148	1.065	1.480	1.725	1.486	1.731	1.493	1.737
152	1.062	1.482	1.723	1.488	1.728	1.495	1.734
156	1.059	1.483	1.720	1.489	1.725	1.496	1.731
158	1.057	1.485	1.718	1.490	1.725	1.497	1.730
160.3	1.055	1.485	1.715	1.491	1.722	1.497	1.727
163	1.053	1.486	1.713	1.493	1.719	1.500	1.725
167	1.050	1.488	1.709	1.494	1.715	1.500	1.721
171	1.046	1.490	1.705	1.495	1.711	1.503	1.718
175	1.043	1.491	1.703	1.497	1.706	1.503	1.713

**Table 6.2**

**Polarisability ( $\alpha_o, \alpha_e$ ) at different temperatures of mixture C<sub>1</sub>  
( $x_{7CBB} = 0.917$ ) by Vuks method**

Temp. in °C	$\lambda = 6907 \text{ \AA}$		$\lambda = 5780 \text{ \AA}$		$\lambda = 5461 \text{ \AA}$	
	$\alpha_o$	$\alpha_e$	$\alpha_o$	$\alpha_e$	$\alpha_o$	$\alpha_e$
120	44.07	76.88	44.56	77.37	45.04	77.86
124	44.31	76.95	44.87	77.48	45.26	78.00
128	44.68	76.99	45.16	77.48	45.64	78.09
130	44.77	76.94	45.34	77.49	45.72	78.09
132	44.91	76.97	45.46	77.50	45.92	78.00
135	45.15	76.97	45.68	77.49	46.16	77.92
139	45.44	76.81	45.93	77.42	46.50	77.81
144	45.89	76.66	46.40	77.08	46.89	77.61
148	46.16	76.61	46.69	77.02	47.19	77.55
152	46.51	76.51	46.99	76.93	47.57	77.43
156	46.75	76.36	47.28	76.78	47.87	77.17
158	47.03	76.18	47.45	76.80	48.05	77.13
160.3	47.18	75.99	47.66	76.57	48.17	76.99
163	47.44	75.83	47.95	76.37	48.54	76.81
167	47.77	75.61	48.28	76.12	48.83	76.62
171	48.16	75.31	48.58	75.87	49.23	76.33
175	48.43	75.26	48.98	75.44	49.47	76.01

$\alpha_o$  &  $\alpha_e$  are in  $10^{-24} \text{ cm}^3$  unit.

**Table 6.3**

**Polarisability ( $\alpha_o, \alpha_e$ ) at different temperatures of mixture C<sub>1</sub>  
( $x_{7CBB} = 0.917$ ) by Neugebauer method**

Temp. in °C	$\lambda = 6907 \text{ \AA}$		$\lambda = 5780 \text{ \AA}$		$\lambda = 5461 \text{ \AA}$	
	$\alpha_o$	$\alpha_e$	$\alpha_o$	$\alpha_e$	$\alpha_o$	$\alpha_e$
120	46.07	72.89	46.57	73.34	47.08	73.79
124	42.29	72.98	46.88	73.47	47.29	73.94
128	46.65	73.05	47.15	73.50	47.66	74.06
130	46.73	73.02	47.32	73.53	47.74	74.06
132	46.87	73.06	47.43	73.55	47.29	74.01
135	47.09	73.08	47.64	73.52	48.14	73.96
139	47.35	72.98	47.87	73.53	48.45	73.90
144	47.77	72.90	48.29	73.29	48.80	73.78
148	48.02	72.89	48.56	73.28	49.08	73.76
152	48.35	72.85	48.84	73.23	49.43	73.70
156	48.56	72.74	49.10	73.14	49.70	73.51
158	48.81	72.61	49.26	73.17	49.86	73.50
160.3	48.94	72.47	49.45	73.00	49.97	73.40
163	49.18	72.36	49.71	72.85	50.31	73.28
167	49.47	72.21	50.00	72.68	50.56	73.15
171	49.82	72.00	50.27	72.50	50.92	72.94
175	50.07	71.98	50.61	72.18	51.12	72.70

$\alpha_o$  &  $\alpha_e$  are in  $10^{-24} \text{ cm}^3$  unit.

**Table 6.4**

**Order parameter  $\langle P_2 \rangle$  of mixture  $C_1(x_{7CBB} = 0.917)$  at different temperatures by Vuks method.**

$$(\alpha_{\parallel} - \alpha_{\perp}) = 45.45 \text{ in } 10^{-24} \text{ cm}^3 \text{ unit.}$$

Temp. in °C	$\lambda = 6907 \text{ \AA}$	$\lambda = 5780 \text{ \AA}$	$\lambda = 5461 \text{ \AA}$	Average
	$\langle P_2 \rangle$	$\langle P_2 \rangle$	$\langle P_2 \rangle$	$\langle P_2 \rangle$
120	0.722	0.722	0.722	0.722
124	0.718	0.717	0.720	0.718
128	0.711	0.708	0.714	0.711
130	0.708	0.707	0.712	0.709
132	0.705	0.705	0.706	0.705
135	0.700	0.698	0.699	0.699
139	0.690	0.693	0.689	0.691
144	0.677	0.675	0.676	0.676
148	0.670	0.667	0.668	0.668
152	0.660	0.659	0.657	0.659
156	0.652	0.649	0.644	0.648
158	0.641	0.646	0.640	0.642
160.3	0.634	0.636	0.634	0.635
163	0.625	0.625	0.622	0.624
167	0.613	0.612	0.611	0.612
171	0.597	0.600	0.596	0.598
175	0.590	0.582	0.584	0.585

**Table 6.5**

**Order parameter  $\langle P_2 \rangle$  of mixture  $C_1$  ( $x_{7CBB} = 0.917$ ) at different temperatures by Neugebauer method.**

$$(\alpha_{\parallel} - \alpha_{\perp}) = 37.05 \text{ in } 10^{-24} \text{ cm}^3 \text{ unit.}$$

Temp. in °C	$\lambda = 6907 \text{ \AA}$	$\lambda = 5780 \text{ \AA}$	$\lambda = 5461 \text{ \AA}$	Average
	$\langle P_2 \rangle$	$\langle P_2 \rangle$	$\langle P_2 \rangle$	$\langle P_2 \rangle$
120	0.724	0.723	0.721	0.723
124	0.720	0.718	0.719	0.719
128	0.713	0.711	0.713	0.712
130	0.710	0.707	0.711	0.709
132	0.707	0.705	0.704	0.705
135	0.702	0.699	0.699	0.699
139	0.692	0.693	0.687	0.691
144	0.678	0.675	0.674	0.676
148	0.671	0.667	0.666	0.668
152	0.661	0.659	0.655	0.658
156	0.653	0.649	0.643	0.648
158	0.642	0.645	0.638	0.642
160.3	0.635	0.636	0.632	0.634
163	0.626	0.625	0.620	0.624
167	0.614	0.612	0.610	0.612
171	0.598	0.600	0.595	0.598
175	0.591	0.580	0.582	0.585

**Table 6.6**

**Mean experimental intensity values  $I(\psi)$ , in arbitrary units, of 7CBB and 12OCB mixture  $C_1$  ( $x_{7CBB} = 0.917$ ) after background correction.**

$\psi$ in deg.	$I(\psi)$ values at different temperatures in degrees				
	125	130	135	140	145
0	3.21	3.31	1.54	1.64	1.01
5	2.87	3.04	1.34	1.54	0.90
10	2.22	2.38	1.01	1.29	0.78
15	1.72	1.72	0.95	1.02	0.64
20	1.08	1.13	0.46	0.79	0.51
25	0.68	0.67	0.29	0.60	0.39
30	0.42	0.38	0.18	0.43	0.29
35	0.26	0.19	0.08	0.30	0.22
40	0.16	0.11	0.04	0.21	0.16
45	0.10	0.09	0.03	0.15	0.11
50	0.08	0.07	0.03	0.11	0.08
55	0.07	0.06	0.03	0.07	0.06
60	0.03	0.04	0.02	0.05	0.04
65	0.02	0.04	0.02	0.04	0.03
70	0.01	0.04	0.01	0.03	0.02
75	0.00	0.03	0.01	0.03	0.01
80	0.00	0.01	0.00	0.02	0.00
85	0.00	0.00	0.00	0.01	0.00
90	0.00	0.00	0.00	0.00	0.00

**Table 6.7**

**Mean experimental intensity values  $I(\psi)$ , in arbitrary units, of 7CBB and 12OCB mixture  $C_1$  ( $x_{7CBB} = 0.917$ ) after background correction.**

$\psi$ in deg.	$I(\psi)$ values at different temperatures in degrees				
	150	155	165	185	195
0	3.01	3.08	2.95	2.80	1.57
5	2.96	3.04	2.93	2.75	1.49
10	2.81	3.01	2.88	2.63	1.33
15	2.57	2.92	2.81	2.45	1.10
20	2.28	2.81	2.67	2.20	0.90
25	1.98	2.62	2.51	1.88	0.70
30	1.64	2.42	2.31	1.58	0.53
35	1.30	2.17	2.34	1.20	0.39
40	0.99	1.92	1.60	0.93	0.28
45	0.73	1.62	1.26	0.73	0.21
50	0.52	1.35	0.94	0.50	0.16
55	0.34	1.04	0.69	0.35	0.13
60	0.22	0.75	0.49	0.23	0.08
65	0.14	0.50	0.31	0.15	0.05
70	0.08	0.35	0.20	0.10	0.04
75	0.05	0.23	0.11	0.08	0.04
80	0.04	0.14	0.05	0.05	0.03
85	0.02	0.05	0.01	0.03	0.01
90	0.00	0.00	0.00	0.00	0.00

**Table 6.8**

**Normalised distribution function values  $f(\beta)$  of 7CBB and 12OCB mixture  $C_1$  ( $x = 0.917$ ).**

$\beta$ in deg.	$f(\beta)$ values at different temperatures in degrees				
	125	130	135	140	145
0	18.828	19.529	22.266	12.064	11.198
5	17.263	17.139	19.898	11.183	10.498
10	12.250	12.329	14.234	9.206	8.625
15	7.999	8.118	8.375	6.856	6.257
20	5.060	5.265	4.515	4.996	4.294
25	3.162	3.360	2.600	3.668	3.086
30	1.861	1.871	1.651	2.322	2.378
35	0.983	0.825	0.950	1.356	1.817
40	0.781	0.332	0.366	0.825	1.208
45	0.249	0.155	0.099	0.488	0.679
50	0.158	0.094	0.036	0.335	0.388
55	0.126	0.083	0.031	0.297	0.277
60	0.111	0.097	0.035	0.246	0.244
65	0.086	0.101	0.045	0.165	0.209
70	0.050	0.074	0.036	0.093	0.128
75	0.006	0.039	0.014	0.043	0.049
80	0.002	0.013	0.00	0.020	0.012
85	0.00	0.005	0.00	0.014	0.004
90	0.00	0.002	0.00	0.012	0.002

**Table 6.9**

**Normalised distribution function values  $f(\beta)$  of 7CBB and 12OCB mixture  $C_1$  ( $x = 0.917$ ).**

$\beta$ in deg.	$f(\beta)$ values at different temperatures in degrees				
	150	155	165	185	195
0	5.388	2.586	3.076	4.716	9.115
5	5.193	2.655	3.097	4.730	8.586
10	4.751	2.767	3.074	4.674	7.300
15	4.284	2.737	2.905	4.385	5.816
20	3.884	2.538	2.677	3.864	4.481
25	3.449	2.332	2.585	3.276	3.359
30	2.839	2.226	2.661	2.730	2.425
35	2.165	2.148	2.652	2.204	1.678
40	1.595	1.935	2.231	1.662	1.135
45	1.153	1.565	1.545	1.159	0.778
50	0.812	1.975	0.999	0.778	0.554
55	0.545	0.942	0.702	0.528	0.406
60	0.340	0.767	0.546	0.365	0.292
65	0.198	0.581	0.404	0.243	0.195
70	0.110	0.353	0.233	0.144	0.119
75	0.060	0.165	0.099	0.077	0.069
80	0.031	0.070	0.036	0.040	0.042
85	0.014	0.030	0.016	0.025	0.029
90	0.009	0.026	0.00	0.021	0.025

**Table 6.10****Variation of  $\langle P_2 \rangle$  and  $\langle P_4 \rangle$  with temperature.****Sample:- 7CBB & 12OCB mixture C<sub>1</sub>**

$$x_{7CBB} = 0.917$$

Temperature in °C	$\langle P_2 \rangle$	$\langle P_4 \rangle$
125	0.790	0.498
130	0.795	0.524
135	0.802	0.534
140	0.693	0.360
145	0.665	0.306
150	0.563 *	----
155	0.395 *	----
165	0.457 *	----
185	0.553	----
195	0.626	0.264

\* data from partially aligned sample, magnetic field not sufficient for alignment.

**Table 6.11**

**Apparent molecular length ( $l_{ap}$ ) or layer thickness ( $d$ ) at different temperatures for mixtures of 7CBB & 12OCB.**

Mix.C <sub>1</sub> ( $x_{7CBB} = 0.917$ )		Mix.C <sub>2</sub> ( $x_{7CBB} = 0.80$ )		Mix.C <sub>3</sub> ( $x_{7CBB} = 0.604$ )	
Temp. in °C	$l_{ap}$ or $d$ in Å	Temp. in °C	$d$ in Å	Temp. in °C	$d$ in Å
120	39.92	110	39.15	100	39.98
125	39.93	120	39.24	110	40.18
130	39.75	130	39.46	120	40.08
135	39.84	140	39.21	130	40.12
140	39.89	150	39.08	140	40.12
145	39.74			150	40.05
150	38.50				
155	37.76				
165	38.62				
175	38.83				
185	38.70				
195	38.52				

**Table 6.12**

**Layer thickness ( d ) at different temperatures for mixtures of 7CBB  
& 12OCB.**

Mix.C <sub>4</sub> (x <sub>7CBB</sub> = 0.502)		Mix.C <sub>5</sub> (x <sub>7CBB</sub> = 0.296)		Mix.C <sub>6</sub> (x <sub>7CBB</sub> = 0.202)	
Temp. in °C	d in Å	Temp. in °C	d in Å	Temp. in °C	d in Å
100	40.59	90	39.72	70	39.79
110	40.38	100	40.12	80	39.53
120	40.35	110	39.85	90	39.66
130	40.86	120	39.92	100	39.79
150	40.45	130	39.92	110	40.12
165	40.72			120	39.78

**Table 6.13**

**Concentration variation of layer thickness (d) for mixture of 7CBB & 12OCB at 120 °C { except point  $x_{7CBB} = 0.917$  ( $\Delta$ ) for which temperature is about 170 °C }.**

$x_{7CBB}$	$l_{ap}$ or $d$ in Å
0.202	39.78
0.296	39.92
0.502	40.35
0.604	40.08
0.800	39.24
0.917	38.66

**References:**

- 1) M. Brodzik and R. Dabrowski, *Liq. Cryst.*, 18, 61 (1995).
- 2) Chapter 2, equation 2.16.
- 3) M. K. Das and R. Paul, *Phase Trans.*, 48, 255 (1994).
- 4) M. K. Das, R. Paul and D. A. Dunmer, *Mol. Cryst. Liq. Cryst.*, 258, 239 (1995).
- 5) S. K. Giri, N. K. Pradhan, R. Paul, S. Paul, P. Mandal, R. Dabrowski, M. Brodzik and K. Czuprynski, *SPIE*, 3319, 149 (1998).
- 6) M. K. Das, S. Paul and R. Paul, *Mol. Cryst. Liq. Cryst.*, 264, 89 (1995).